

## Sinusoidal phase-modulating Fizeau interferometer using phase-conjugate wave

Osami Sasaki, Xiangzhao Wang, Yuuichi Takebayashi, Takamasa Suzuki

Niigata University, Faculty of Engineering  
8050 Ikarashi 2, Niigata-shi 950-21, Japan

### Abstract

We propose a sinusoidal phase-modulating Fizeau interferometer using self-pumped conjugate wave for surface profile measurements. The interferometer is self-referencing and free from the effects of the axial movements of object surfaces. The characteristics of the interferometer are made clear through the surface measurement of a diamond-turned aluminum disk. For large-size objects, the size of the plate glass can be much smaller than that of the object. The small-size plate glass provides the accurate sinusoidal phase modulation easily. We also propose the method of absolute measurement to eliminate the undesirable phase distribution caused by aberration of the lenses. It is shown through the surface profile measurements of a mirror that the interferometer and the method of absolute measurement are useful for large-size objects.

### 1. Introduction

Fizeau interferometers have been used widely because their configurations of common path provide stable and easy measurements of surface profiles of large-diameter objects. Fringe scanning interferometry, heterodyne interferometry<sup>1)</sup> and sinusoidal phase-modulating (SPM) interferometry<sup>2)</sup> are incorporated in Fizeau interferometers to get a high measurement accuracy.

Recently, there has been a lot of interests in applications of a phase-conjugate wave to interferometers. The phase-conjugate Fizeau interferometer<sup>3)</sup> was proposed where a BaTiO<sub>3</sub> self-pumped phase-conjugator is applied to the Fizeau interferometer. An incident light wave whose phase distribution is to be measured interferes with its phase-conjugate wavefront. Therefore, this interferometer does not need another reference wave, that is, the interferometer is self-referencing. The resultant interference pattern directly illustrates the phase distribution of the wavefront of the incident light. However, the interference pattern is not processed in the same way as that used in fringe scanning or SPM interferometers, so the phase distribution of the incident wave can not be obtained with a high accuracy. In addition, the interferometer was not constructed to measure surface profiles of objects.

In this paper we apply the phase-conjugate Fizeau interferometer to surface profile measurements of objects. The light reflected by the object is transformed with two lenses to make a reduced field on a plate glass whose complex amplitude distribution is identical to that of the original field. The reduced field is considered as the object field, and the self-pumped phase-conjugate wave of the object wave is considered as the reference wave. The object wave is phase-modulated by vibrating the plate glass sinusoidally with piezoelectric transducers (PZTs). A CCD image sensor is used to detect the time-varying interference signal. The surface profile of the object is obtained with the signal processing employed in sinusoidal phase modulating interferometry<sup>4,5)</sup>.

The new interferometer is based upon the combination of the phase-conjugate Fizeau interferometer and sinusoidal phase modulating interferometry, and has advantages of both of them. The interferometer is free of the phase fluctuations of the object wave caused by spatially uniform movements of the object because spatially uniform phase changes of the object wave is not reversed on the self-pumped phase-conjugate wave<sup>6)</sup>. Since the object wave is reduced on the plate glass, the dimensions of the plate glass can be much

smaller than those of the objects. This feature makes it easy to carry out exact sinusoidal phase modulation for large-diameter objects.

The phase-conjugate Fizeau interferometer for surface profile measurements, however, has a weak point. Undesirable phase distributions caused by aberration of lenses and roughness of optical surfaces are added to a phase distribution that represents the surface profile of the object. We propose a method of absolute measurement to eliminate the undesirable phase distribution. We measure three phase distributions before and after giving the object surface a displacement in horizontal and vertical directions. From these three phase distributions the surface profile of the object can be calculated absolutely. This method of absolute measurement is applied to the phase-conjugate Fizeau interferometer.

We first describe the principle of the new SPM Fizeau interferometer with a self-pumped conjugate wave for surface profile measurements. Through the measurements of the surface profile of a diamond-turned aluminum disk, the characteristics of the interferometer are made clear. Next the configuration of the interferometer is modified for large-diameter objects. We describe the principle of the absolute measurement. Finally, through the measurement of a mirror, it is shown that the interferometer and the absolute measurement is useful for large -diameter objects.

## 2. Principle

### A. Interferometer

Figure 1 shows a SPM Fizeau interferometer using a phase conjugate wave. A laser beam collimated with lenses L1 and L2 is incident on a surface of the object through a beam splitter BS1. The object field generated by the illumination of the beam is written as

$$U_o(x)=\exp[2jkr(x)] , \quad (1)$$

where  $r(x)$  is the surface profile of the object,  $x$  is a coordinate on the object, and  $k$  is the wave number. The beam reflected by the object is bent at right angles by the beam splitter BS1. Lenses L3 and L4 form an object field in the image space at the surface of the plate glass. The transmitted beam through the plate glass is focussed with a lens L6 into the self-pumped conjugator of a BaTiO<sub>3</sub> crystal, which produces a phase conjugate wave. The phase conjugate wave interferes with the object wave on the plate glass. In this interferometer, the phase conjugate wave is considered as a reference wave, and the beam reflected by the plate glass is considered as the object wave.

The sinusoidal phase modulating interferometry is used to obtain the phase distribution of the interference pattern. To phase-modulate the object beam, the plate glass is sinusoidally vibrated with PZTs. The vibration of the plate glass is expressed by

$$A(t)=a \cos(\omega_c t+\theta) . \quad (2)$$

The reference and object fields on the plate glass can be written as

$$U_{1r}(x')=R\exp[-2jkr(x')] , \quad (3)$$

$$U_{1o}(x')=\exp[2jkr(x')+Z\cos(\omega_c t+\theta)] , \quad (4)$$

where  $R$  is the phase-conjugate reflectivity,  $Z=(4\pi/\lambda)a$ , and  $x'$  is a coordinate on the plate glass. The lens L5 images these fields on a CCD image sensor. The interference pattern generated from  $U_{1r}(x')$  and  $U_{1o}(x')$  on the CCD image sensor is expressed as

$$I(x'',t)=1+R^2+2R\cos[Z\cos(\omega_c t+\theta)+\alpha], \quad (5)$$

where

$$\alpha=(8\pi/\lambda)r(x''), \quad (6)$$

and  $x''$  is a coordinate on the CCD image sensor. The ac-component of the interference signal

$$S(x'',t)=S_0\cos[Z\cos(\omega_c t+\theta)+\alpha] \quad (7)$$

is detected with the CCD image sensor. The phase  $\alpha$  is obtained with the Fourier transform method<sup>4)</sup>. The surface profile of the object is given by  $r(x'')=(\lambda/8\pi)\alpha(x'')$ .

When the object is moved in parallel with the optical axis, the phase of  $U_o(x)$  or  $U_{1o}(x')$  changes uniformly in space. The phase of  $U_{1r}(x')$  gets the same change as the phase of the  $U_{1o}(x')$  due to the characteristics of self-pumped phase conjugator<sup>6)</sup>. So the interference pattern is not affected by the time-varying phase change of the object wave. The interferometer has a special feature that it is completely free of the disturbance in axial movements of objects. In addition, the sensitivity of this interferometer is twice as high as that of conventional interferometers, as shown in Eq.(6).

### B. Formation of the object field in image space

When the interferometer shown in Fig.1 is used to measure the surface profile of an object, it is a key point to make the object field in the image space on the plate glass. In other words, the relationship between the positions of the plate glass and the object surfaces is very important. If the object is not placed on the right position, the measurement errors will occur.

To find the relationship between the positions of the object fields in object and image spaces, transformation of the field with the lenses L3 and L4 is shown in Fig.2. The back focal point of the lens L3 coincides with the front focal point of the lens L4. The  $f_3$  and  $f_4$  are the focal lengths of the two lenses respectively. The  $l_1$  and  $l_2$  are the distances between the two lenses and corresponding object fields, respectively. We consider two rays of light which propagate at an angle of  $\theta_1$  with the optical axis from the object field plane and front focal point of the lens L<sub>3</sub>. These two rays are reach in image space at an angle of  $\theta_2$  with the optical axis as shown in Fig.2. The following relations are obtained from the propagation of the two rays;

$$f_3 \tan\theta_1 = f_4 \tan\theta_2, \quad (8)$$

$$l_2 \tan\theta_2 = f_3 \tan\theta_1 - (f_4/f_3)(l_1 - f_3) \tan\theta_1. \quad (9)$$

From (8) and (9), the position of the object field in image space is given by

$$l_2 = f_4 - (f_4/f_3)^2(l_1 - f_3). \quad (10)$$

When the distances  $l_1$  and  $l_2$  satisfy Eq.(10), the same phase distribution as the object surface will be formed on the plate glass.

### 3. Measurement of 1-D surface profiles.

The experimental setup is shown in Fig.1. The light source is an argon-ion laser with wavelength  $\lambda=514.5\text{nm}$ . The lenses L3 and L4 have the same focal length  $f_3=f_4=100\text{mm}$ . The object is a diamond-turned aluminum disk, and the distance  $l_1$  is adjusted to  $f_3$ . In order to make the same phase distribution as the disk

surface on the plate glass, the distance  $l_2$  is adjusted to  $f_4$ . A surface of the plate glass is coated with an antireflection layer, and the other surface reflects an object wave. The plate glass is attached to three PZTs. The object wave is phase-modulated by vibrating sinusoidally the plate glass with PZTs. The BaTiO<sub>3</sub> crystal has a dimension of 5×5×5mm. The interference pattern on the plate glass is imaged onto a 1-D CCD image sensor by a lens L<sub>5</sub> of focal length  $f_5=70\text{mm}$ .

A CCD image sensor with a pixel size of 9×14μm and the pixel interval of 14μm is employed. The 28 elements of the CCD image sensor receive the interference signal and the remaining ones are covered with black paper. The image of the disk surface is formed on the CCD image sensor with a magnification of 2.5, hence the spatial interval of the measuring points is 5.6μm. The frequency of the sinusoidal phase modulation  $\omega_c/2\pi$  is 187Hz. The output of the CCD image sensor is A-D converted to be stored in a computer, and the surface profile is obtained.

Fig.3 shows the measured surface profile of the object. The peak-to-peak roughness of the measured surface is ~100nm and its period is ~50μm. The measured surface profile agrees with the surface profile of Fig.4 measured with a Talystep instrument. The measurement of the same disk surface was repeated after an interval of a few minutes. The measurement repeatability was below 0.5nm.

The effect of object's positions on the measurements was examined experimentally. The object surface was moved backwards and forwards from the right position by 0.4mm, that is, position errors of  $\Delta l=0.4\text{mm}$  and  $-0.4\text{mm}$  were given. The results are shown in Fig.5. It is found that there is a little change in the measured cutting pitch while the peak-to-peak roughness obviously decreases with the increase of the position error. If we expect that the measurement error of the peak-to-peak value is less than 80%, the position error must be less than 0.2mm for the disk surface employed.

#### 4. Interferometer for large-diameter objects

We modify the configuration of the interferometer shown in Fig.1 to measure a large-diameter object. The new configuration of the interferometer is shown in Fig.6. Lenses L<sub>0</sub> and L<sub>1</sub> make a collimated beam, and lenses L<sub>1</sub> and L<sub>2</sub> form an object field in the image space on the plate glass. The dimensions of the plate glass is smaller than those of the object. The reduced scale of the dimensions is the ratio of the focal lengths of the lenses L<sub>1</sub> and L<sub>2</sub>. A 2-D CCD image sensor detects the interference signal.

When the diameter of an object is large, the diameter of the lens L<sub>1</sub> also becomes large and has aberration. Then an undesirable phase distribution is introduced by the aberrating lens. In this case the phase-conjugate interferometer detects the phase distribution  $\alpha = \beta + \phi$ , where  $\beta$  is the phase distribution that represents the surface profile of the object, and  $\phi$  is the undesirable phase distribution.

We propose a method for eliminating the undesirable phase distribution to measure absolutely flatness of the object

#### 5. Absolute measurement

First, we measure the phase distribution

$$\alpha(i,j) = \beta(i,j) + \phi(i,j) , \quad (11)$$

where a point (i,j) indicates a measuring point. Secondly, we move the object in horizontal direction or the x-axis direction by the interval of the measuring points in the x-axis direction. Then the measured phase distribution is written as

$$\alpha_h(i,j) = \beta(i+1,j) + \phi(i,j) . \quad (12)$$

Thirdly, we move the object in vertical direction or the y-axis direction by the interval of the measuring points in the y-axis direction. Then we measure the phase distribution

$$\alpha_v(i,j) = \beta(i,j+1) + \phi(i,j) . \quad (13)$$

Finally, we obtain the following values from the three measured values  $\alpha$ ,  $\alpha_h$ , and  $\alpha_v$  ;

$$\begin{aligned} h(i,j) &= \alpha_h(i,j) - \alpha(i,j) \\ &= \beta(i+1,j) - \beta(i,j) , \end{aligned} \quad (14)$$

$$\begin{aligned} v(i,j) &= \alpha_v(i,j) - \alpha(i,j) \\ &= \beta(i,j+1) - \beta(i,j) . \end{aligned} \quad (15)$$

These values are the differential values of  $\beta(i,j)$  according to  $i$  and  $j$ , respectively, and they do not contain the undesirable phase distribution  $\phi$ .

Next step is to calculate the phase  $\beta$  from the  $h$  and  $v$ . We consider a simple case of  $3 \times 3$  measuring points, that is,  $i, j = 1 \sim 3$ . The relationship between  $h$ ,  $v$ , and  $\beta$  is given by the matrix representation

$$\begin{bmatrix} h(1,1) \\ h(2,1) \\ h(1,2) \\ h(2,2) \\ h(1,3) \\ h(2,3) \\ v(1,1) \\ v(2,1) \\ v(3,1) \\ v(1,2) \\ v(2,2) \\ v(3,2) \end{bmatrix} = \begin{bmatrix} -1 & 1 & 0 & 0 & 0 & 0 & 0 & 0 & 0 \\ 0 & -1 & 1 & 0 & 0 & 0 & 0 & 0 & 0 \\ 0 & 0 & 0 & -1 & 1 & 0 & 0 & 0 & 0 \\ 0 & 0 & 0 & 0 & -1 & 1 & 0 & 0 & 0 \\ 0 & 0 & 0 & 0 & 0 & 0 & -1 & 1 & 0 \\ 0 & 0 & 0 & 0 & 0 & 0 & 0 & -1 & 1 \\ -1 & 0 & 0 & 1 & 0 & 0 & 0 & 0 & 0 \\ 0 & -1 & 0 & 0 & 1 & 0 & 0 & 0 & 0 \\ 0 & 0 & -1 & 0 & 0 & 1 & 0 & 0 & 0 \\ 0 & 0 & 0 & -1 & 0 & 0 & 1 & 0 & 0 \\ 0 & 0 & 0 & 0 & -1 & 0 & 0 & 1 & 0 \\ 0 & 0 & 0 & 0 & 0 & -1 & 0 & 0 & 1 \end{bmatrix} \begin{bmatrix} \beta(1,1) \\ \beta(2,1) \\ \beta(3,1) \\ \beta(1,2) \\ \beta(2,2) \\ \beta(3,2) \\ \beta(1,3) \\ \beta(2,3) \\ \beta(3,3) \end{bmatrix} \quad (16)$$

Generally, Eq.(16) is written as

$$\boldsymbol{\gamma} = A\boldsymbol{\beta} , \quad (17)$$

where the elements of the vector  $\boldsymbol{\gamma}$  are  $h$  and  $v$ . When the measuring points are  $L \times M$  points, the vector  $\boldsymbol{\beta}$  has  $LM$  elements and the vector  $\boldsymbol{\gamma}$  has  $2LM - (L+M)$  elements. So we can solve the linear equation of Eq.(17) for the unknowns  $\boldsymbol{\beta}$ . We obtain a solution  $\boldsymbol{\beta}$  by minimizing the objective function  $B = \|\boldsymbol{\gamma} - A\boldsymbol{\beta}\|^2$  with the conjugate gradient method.

Computer simulations show that this method of solving the linear equation gives a good solution. When the measured values  $\alpha$ ,  $\alpha_h$ , and  $\alpha_v$  contain noises, this method does not increase the noises in the solution.

## 6. Absolute measurements of 2-D surface profiles

We measured the surface profile of a mirror of a diameter 20 mm. The lens  $L_0$  is a 40 $\times$ microscopic objective lens, and the focal lengths of lenses  $L_1$  and  $L_2$  are 250mm and 70mm, respectively. The object is

placed at 250mm from the lens  $L_1$ .

The surface profile was measured through the integrating-bucket method<sup>5)</sup>. The spatial intervals of the measuring points in the two directions were 1.0mm and 0.9mm, respectively. The 20×20 elements of the CCD image sensor were used to detect the intensity distribution of the light. The frequency of the sinusoidal phase modulation is 120Hz.

Figures 7(a), (b), and (c) show the surface profiles of the mirror obtained from the three measured phase distribution  $\alpha$ ,  $\alpha_h$ , and  $\alpha_v$ , respectively. Because these distributions contain the undesirable phase  $\phi$ , the root mean square (rms) of the height distribution and the peak-valley distance (P-V) are large. The rms and P-V values are about 25 nm and 120 nm, respectively, in these results. The result of absolute measurement obtained from the three surface profiles of Figs.7(a), (b), and (c) is shown in Fig.7(d). The rms and P-V values are 7.4 nm and 37 nm, respectively. These results make it clear that we can eliminate the undesirable phase and achieve the absolute measurement with the method proposed.

## 7. Conclusions

We have demonstrated a sinusoidal phase-modulating Fizeau interferometer using self-pumped conjugate wave generated with BaTiO<sub>3</sub> crystal for surface profile measurements. This interferometer is self-referencing and is free from the phase fluctuations of the object wave caused by the spatially uniform movements of the object. The characteristics of the interferometer were made clear through the surface measurement of a diamond-turned aluminum disk. For large-size objects, the size of the plate glass need not be equal to that of the object. The small-size plate glass provides the accurate sinusoidal phase modulation easily. We also have proposed the method of absolute measurement to eliminate the undesirable phase distribution caused by aberration of the lenses. It was shown through the surface profile measurements of a mirror that the interferometer and the method of absolute measurement were useful for large-size objects.

## References

1. T. H. Barnes, "Heterodyne Fizeau Interferometer for Testing Flat Surface," *Appl. Opt.* 26, 2084-2809(1987).
2. O. Sasaki, T. Okamura, and T. Nakamura, "Sinusoidal Phase Modulating Fizeau Interferometer," *Appl. Opt.* 29, 512-515(1990).
3. D. J. Gauthier and R. W. Boyd, "Phase-conjugate Fizeau Interferometer," *Opt. Lett.* 14, 323-325(1989).
4. O. Sasaki and H. Okazaki, "Sinusoidal Phase Modulating Interferometry for Surface Profile Measurement," *Appl. Opt.* 25, 3137-3140(1986).
5. O. Sasaki, H. Okazaki, and M. Sakai, "Sinusoidal Phase Modulating Interferometer Using Integrating-Bucket Method," *Appl. Opt.* 26, 1089-1093(1987).
6. Y. Tomita, R. Yahalom and A. Yariv, "Phase Shift and Cross Talk of a Self-Pumped Phase-Conjugate Mirror," *Opt. Comm.* 73, 413-418(1989).

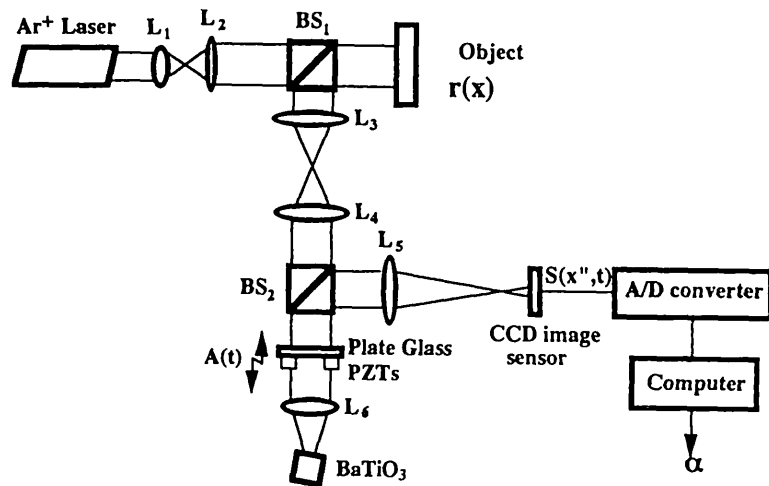


Fig. 1. SPM Fizeau interferometer using self-pumped conjugate wave.

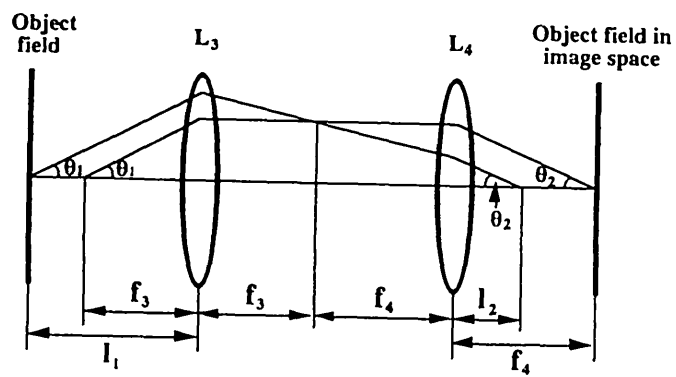


Fig. 2. Formation of the object field in image space.

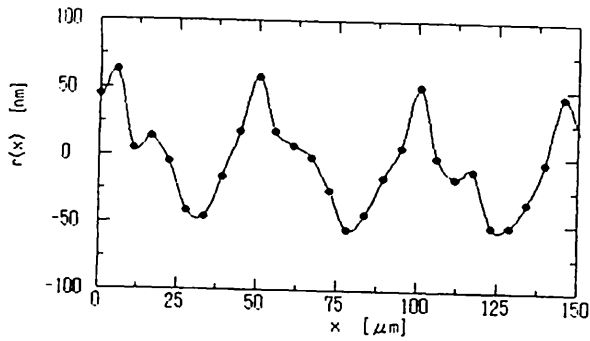


Fig. 3. Measured surface profile of a diamond-turned aluminum disk.

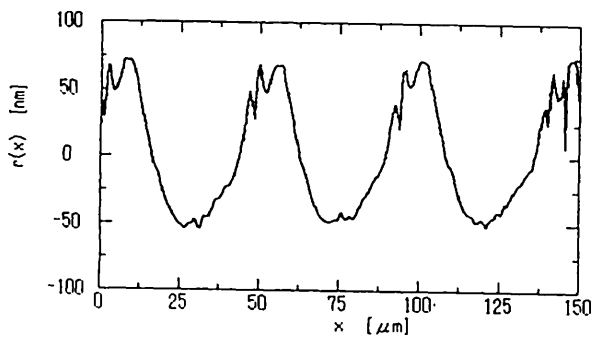
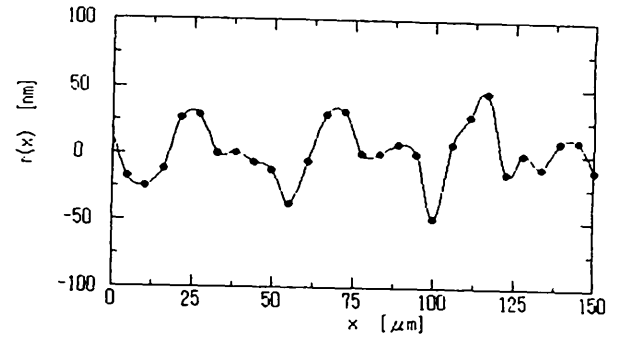
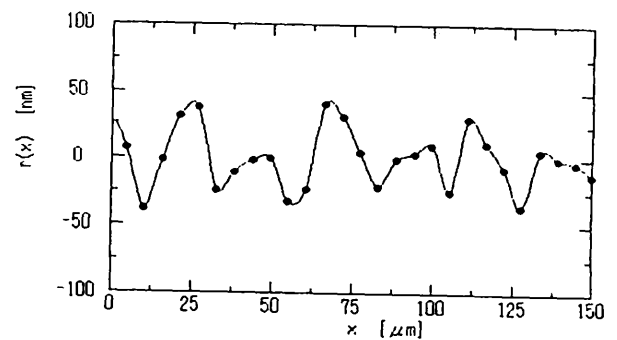


Fig. 4. Surface profile of a diamond-turned aluminum disk measured with a Talystep instrument.



(a)



(b)

Fig. 5. Surface profiles of a diamond-turned aluminum disk measured at (a) the position errors  $\Delta l = 0.4$  mm and (b)  $\Delta l = -0.4$  mm.

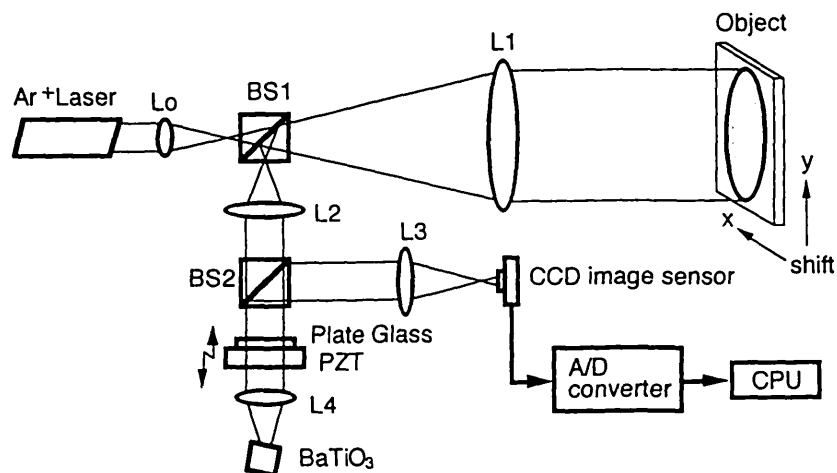
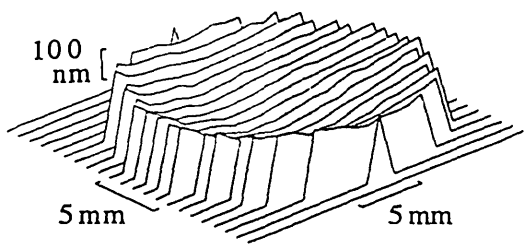
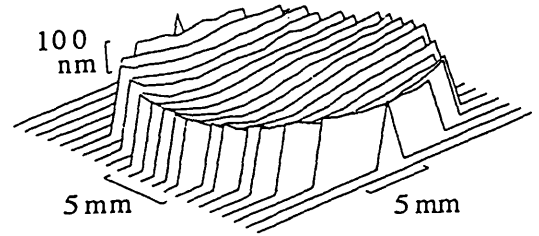


Fig. 6. SPM Fizeau interferometer using phase conjugate wave for surface profile measurements of large-diameter objects.

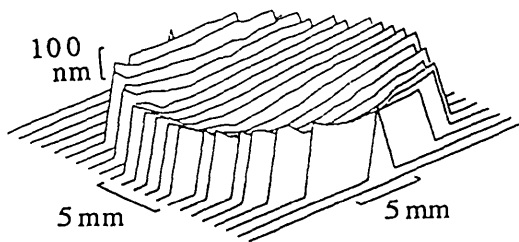




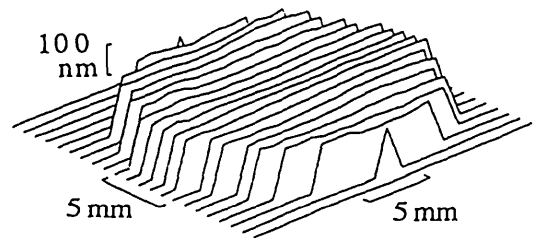
(a)



(b)



(c)



(d)

Fig. 7. Measured surface profiles of a 20mm diameter mirror obtained from (a)  $\alpha$ , (b)  $\alpha_h$ , (c)  $\alpha_v$ , and with (d) the absolute measurement.

**In-Position Optical Surface Measurement  
for X-Ray Projection Lithography Optics**  
-- Theory and Simulation --

Eiichi Seya, Minoru Hidaka, Masaaki Ito, Sohichi Katagiri and Eiji Takeda

Central Research Lab., Hitachi Ltd.  
1-280, Higashi-Koigakubo, Kokubunji, Tokyo 185, Japan  
telephone +81-423-23-1111, fax +81-423-27-7706

**ABSTRACT**

A technique is proposed to measure X-ray projection optics. Simultaneous linear equations are derived from the wavefront distortions to obtain form errors of optical surfaces discretely. Simulations proved that the arithmetic operation errors are small enough to achieve nanometer level accuracy. This technique will be effective to testify aspheric reflectors, as well as the reflector misalignments. It will also be able to apply to adaptive optics compensating for thermal deformation effects or drifts on the exposure system.

**INTRODUCTION**

X-ray projection lithography will be potential in the future productions of semiconductors having a pattern size of 0.1  $\mu\text{m}$  or less. Technical difficulties to realize X-ray projection lithography are mainly on the projection optics construction, especially on the reflecting optical surface forming. One reason for the difficulties is that the wavefront distortion of the optics should be less than 3 nm to achieve a resolution of 0.1  $\mu\text{m}$ . Another is that the reflector surfaces should be aspheric to lessen the total number of reflectors included in the optics.

Aspheric testing techniques are essential to achieve the reflectors. Interferometry is advantageous to this purpose because of its simultaneity. However, it is not easy to achieve nanometer-level absolute accuracy due to return path shift problem on aspheric measurements.

The technique presented here has its basis on the wavefront distortion measurements. Simultaneous linear equations derived from the measured distortions obtain the errors on the discrete surfaces. This technique avoids effects of the problem described above because it refers directly to the optical characteristics we intend to realize.

**TECHNICAL PRINCIPLE**

Our approach to form the aspheric surfaces consists of two steps. The first step is aspheric generation by pressure-controlled multi-tool polishing. The second step is improvement by profile-controlled local deposition. Each step is a form-feedback operation that repeats forming and measurement in turn. The final accuracy by this approach certainly depends mostly on the measurement accuracy.

We can achieve measurement repeatability better than 2 nm with sub-fringe interferometry. The absolute measurement accuracy is better than 10 nm with reference error compensation<sup>1)</sup>. However, aspheric measurement accuracy is worse compared with spherical measurements due to the return path shift.

Figure 1 shows an example of wavefront measurement with an interferometer. The measured result is